Front. Mech. Eng. 2018, 13(2): 311–322
https://doi.org/10.1007/s11465-018-0494-x

REVIEW ARTICLE

Weihua ZHANG, Dong ZOU, Mengying TAN, Ning ZHOU, Ruiping LI, Guiming MEI

Review of pantograph and catenary interaction

© Higher Education Press and Springer-Verlag GmbH Germany, part of Springer Nature 2018

Abstract The application of electrified railway directly promotes relevant studies on pantograph-catenary interaction. With the increase of train running speed, the operating conditions for pantograph and catenary have become increasingly complex. This paper reviews the related achievements contributed by groups and institutions around the world. This article specifically focuses on three aspects: The dynamic characteristics of the pantograph and catenary components, the systems' dynamic properties, and the environmental influences on the pantograph-catenary interaction. In accordance with the existing studies, future research may prioritize the task of identifying the mechanism of contact force variation. This kind of study can be carried out by simplifying the pantograph-catenary interaction into a moving load problem and utilizing the theory of matching mechanical impedance. In addition, developing a computational platform that accommodates environmental interferences and multi-field coupling effects is necessary in order to further explore applications based on fundamental studies.

Keywords electrified railway, pantograph and catenary interaction, contact force variation, moving load problem, mechanical impedance, multi-field

1 Introduction

The performance of a high-speed train (HST) is subjected to the influences arising from the wheel-rail interaction, the pantograph-catenary interaction, and the aerodynamic resistances (Fig. 1). As one of the basic mechanics problems of the HST dynamics, the pantograph-catenary interaction plays an important role in HST operation, because it supplies the electric resource of traction power for electric rail vehicles. Thus, the operational stability of an HST is highly dependent upon the performance of the pantograph and catenary system.

Figure 2 illustrates two types of catenary system: Simple and stitched. Figure 2(a) presents the simple catenary consisting of a messenger wire, a contact wire, droppers, registration arms, and support brackets. The messenger wire, which is suspended by the brackets, is connected to the contact wire via equally or non-equally placed droppers. The registration arms, installed on the support brackets, are used to clamp the contact wire to form a zig-zag pattern above the centerline of the tracks. Compared with the simple catenary, an elastic dropper is installed between two adjacent spans for the stitched catenary (Fig. 2(b)). This kind of improvement not only increases the uniformity of the vertical elasticity within a catenary span but also adds energy transmission passage between adjacent spans. When a stitched catenary is subjected to external excitations, the mechanical energy is transmitted to the whole catenary rapidly in the form of an elastic wave, thereby reducing the interruption from local elastic wave to the contact state between the pantograph and catenary. As a result, the performance of the stitched catenary is always favorable. However, compared with the simple one, the stitched catenary has less popularity and application because of the complexity of its construction and maintenance.

The pantograph can be classified into three different types: Four-bar linkage, diamond, and T-type pantographs. The diamond pantograph (Fig. 3(a)) is not commonly used because it has the potential to break the catenary when it is out of order. The T-type pantograph (Fig. 3(b)) has a simple structure with good aerodynamic performance and is mainly used in the railway lines that prefer a low working height, such as the Japanese Shinkansen. The most popular pantograph consists of a four-bar linkage, a balance bar, and a current collector (Fig. 3(c)). The balance bar connects the current collector to the four-bar linkage and keeps it moving in a vertical trajectory. As the constraint between the current collector and the balance bar can be designed with different types, the four-bar linkage pantograph has many variations and has been widely used

Received April 28, 2017; accepted September 27, 2017

Weihua ZHANG, Dong ZOU (✉), Mengying TAN, Ning ZHOU, Ruiping LI, Guiming MEI
State Key Laboratory of Traction Power, Southwest Jiao Tong University, Chengdu 610031, China
E-mail: zdong_hn@163.com

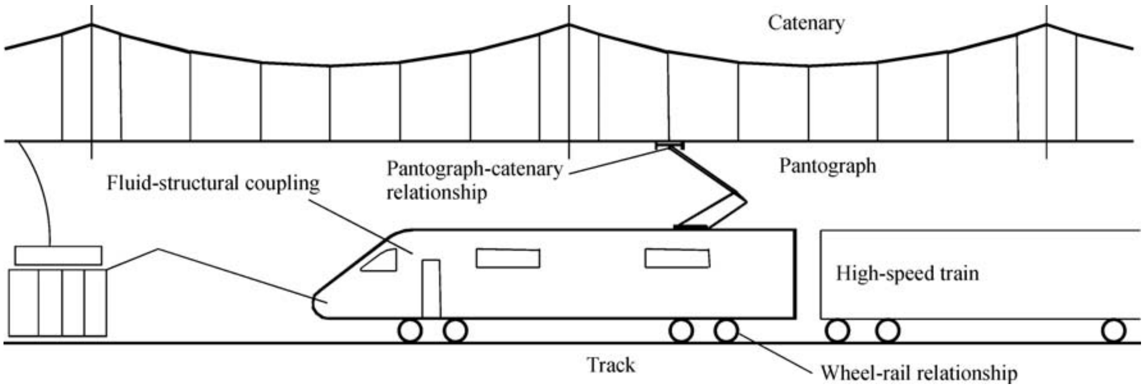

Fig. 1 Three basic mechanics problems in high-speed railway [1]

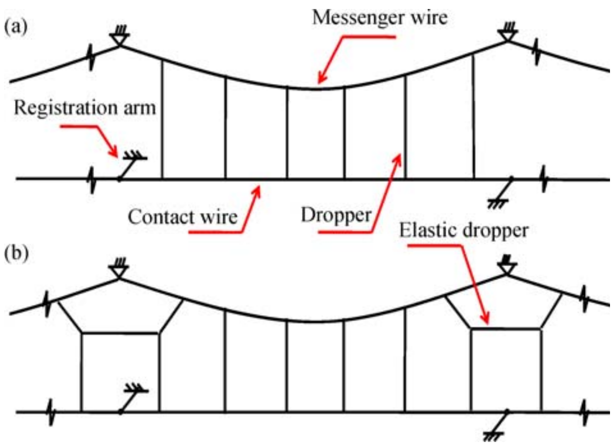

Fig. 2 Different catenary systems. (a) Simple catenary; (b) stitched catenary

all over the world. Actually, regardless of the type of pantograph, it is generally used to lift the current collector to the desirable working height, thus putting it into contact with the catenary wire and obtaining the current transmission.

Actually, the pantograph and catenary interact in a multi-physical environment. Many types of energy transformation occur on the contact interface, including mechanical, heat, and electric energies. Consequently, the performance of the system depends on the multi-coupled interactions among the mechanical properties (general and fluid mechanics) and electrical and thermal effects. However, no matter what the subject is, a stable contact state between the pantograph and catenary is preferred. As the stability of the contact state depends on the lift force in the working height of a pantograph, good mechanical properties serve as the bases of operation of the pantograph-catenary system. In this paper, we do not pay attention to the content outside the pantograph and catenary dynamics, such as the electrical contact [2–6], friction and wear [7–10], heat effect [11], and simulation and test technology of the pantograph-catenary system. More details can be seen from the relevant reviews [12,13].

When a moving pantograph passes through a discontinuous node upon the contact wire, i.e., the clamp position, this can lead to a transition radiation of the elastic wave on the catenary [14]. This kind of elastic wave conversely interrupts the vibration of the moving pantograph, resulting in the dynamic interaction between the pantograph and catenary. In addition, the ambient wind and the vehicle body movements caused by the degraded track

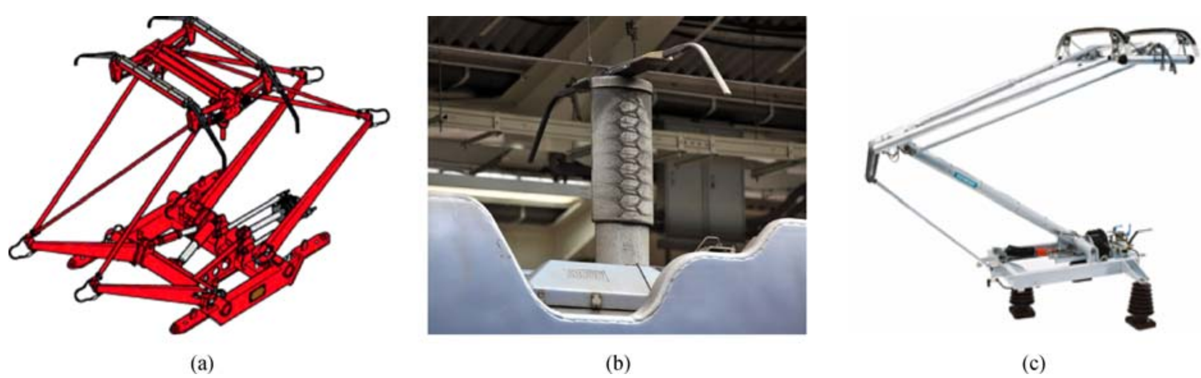

Fig. 3 Different types of pantograph. (a) Diamond pantograph-ATR90; (b) T-type pantograph-Shinkansen Serie 500; (c) four-bar linkage pantograph-SSS400

may also influence the pantograph and catenary dynamics. Therefore, the first section, which focuses on the catenary and pantograph components, presents a comprehensive review of their influences on the system performance. The second section introduces the basic characteristics of the catenary and pantograph, including the properties of wave propagation and the responses to the multiple-pantograph operation. The third section briefly discusses the effects of environmental factors to the pantograph-catenary system. Finally, we give some prospects on the studies of the pantograph-catenary interaction.

2 Dynamic characteristics of the catenary and pantograph components

Both the catenary and the pantograph have various types and are made up of complex components. For the catenary, the droppers and registration arms directly determine the equilibrium position of the contact wire and consequently affect the vertical elasticity within the catenary span. The section insulator is the location wherein the quality of current collection always degrades. Regarding the pantograph, the suspension components and the current collector are the key factors that affect the performance of the pantograph.

2.1 Catenary components

In the static aspect, the arrangement of droppers determines the vertical elasticity of the catenary within a span. While in the dynamic aspect, the dropper's slackening caused by the moving pantograph shocks the internal force of the dropper with large amplitude. This oscillating force plays a critical role in the fatigue life of the dropper. Moreover, the force can also interrupt the contact state between the pantograph and catenary, conversely.

To investigate the effects of the dropper slackening to the contact force between a moving oscillator and a hanger-supported beam, Lee and Chung [15] conducted several profound studies, with consideration of both the slackness and non-slackness hanger models. The authors set the tension of the beam and used the moving speed of the oscillator, the hanger stiffness, the suspension stiffness, and the mass of the oscillator as the variable parameters, and found that the contact force computed with the slackness model is smoother than that computed with the non-slackness model. On the contrary, the amount of discrepancy depends on the moving speed of the oscillator and the tension of the beam with the highest sensitivity compared with other parameters.

Lopez-Garcia et al. [16] focused on the dropper slackening effects to the vertical stiffness of a real catenary. The stiffness is found to have a local maximum around the droppers in a complete catenary span. The same results can be seen in both the slackness (referred as taut-slack dropper) and non-slackness (referred as only taut dropper) dropper models. However, the slackening of the taut-slack dropper can smooth the local maximum compared with the only taut dropper. By applying the moving forces to the catenary with different amplitudes and conducting static analysis, he compared the relative difference of the catenary stiffness between these two dropper models. Figure 4 shows that the stiffness is the same when the force is below 100 N, and if the force keeps increasing; in comparison, the difference presents and reaches 16% when the force is 250 N.

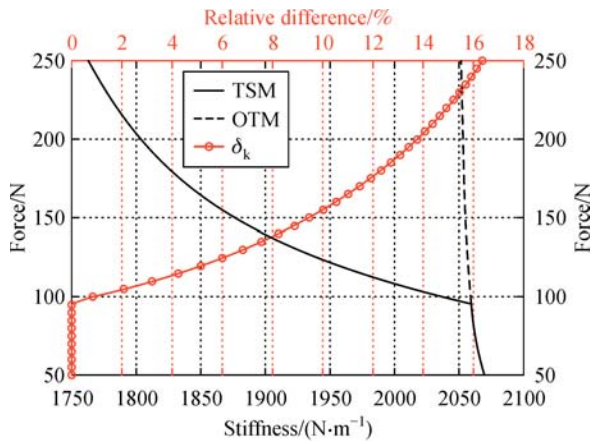

Fig. 4 Comparison of catenary stiffness between dropper models with and without slackening

To investigate the effects of dropper slackening on the pantograph-catenary interaction, Cho et al. [17,18] studied the variation of contact force between the pantograph and catenary by changing the amplitude of the uplift force applied to the pantograph and adjusting the moving speed of the pantograph. A relatively large uplift force is found to slack the droppers and consequently reduce the catenary stiffness. However, the reduced stiffness just smooths out the contact force variation when the moving speed is equivalent to 50% of the catenary wave propagation speed. If the speed increases to 70% of the wave propagation speed, then the variation of the contact force increases drastically. Thus, the authors conclude that, unless the wave reflection becomes a major cause of contact loss, the increased uplift force can reduce the variation of the contact force because of the dropper slackening.

When the pantograph passes through a registration arm, the stress of the contact wire increases and oscillates drastically. To clarify this phenomenon, Morikawa [19] theoretically analyzed the stress level when different types of registration arms interact with a moving pantograph, and reported that the constraint type of the registration arm has great influences on the stress magnitude.

In the severe cold region, the catenary tension changes occasionally due to the varying temperature. Amari et al. [20] found that, when the temperature decreases to 14 °C, the tension of the messenger wire can increase from 1.2 to 1.5 kN (Fig. 5(a)), in which case the quality of the current collection is severely affected. To prevent this kind of tension variation and to improve the performance of the catenary, Amari et al. [20] built a supporting pulley of messenger wire with optimized resistance parameters.

As a common device, the section insulator is used to separate the catenary into different sections. Sugahara [21] found that the difference of the sliding surface level at the ends of the section insulator can potentially induce a fatigue failure of the catenary.

2.2 Pantograph components

Regarding the components of the pantograph, the current collector suspended at the pantograph frame is the component that comes into direct contact with the catenary. Because the elasticity of the pantograph frame mainly contributes to a relatively high frequency, it is the type of current collector and its suspension properties that determine the basic frequency response characteristic of a pantograph.

To clarify the most sensitive suspension parameters, Park et al. [22] and Kim et al. [23,24] conducted several studies and presented several conclusions. They modeled the catenary by using a spring with variable properties, which correspond to the stiffness of the catenary, and simplified the pantograph into a spring-mass-stiffness system. After constructing the table of the orthogonal array of design parameters, they then used the sensitivity of parameters and the signal-to-noise ratio to assess the pantograph performance when the catenary span length and the pantograph running speed change. Referring to their results, the mass of current collector, the stiffness between the pantograph frame and crossbar, and the damping between the pantograph frame and the vehicle roof have been proven to be the most sensitive parameters. On the basis of their conclusions, Pombo and Ambrósio [25] also conducted some contributive works to study the influences of a pantograph's structural parameters on the system performance.

To improve the quality of the current collection, Yoshitaka and Ikeda [26] proposed a new technology for the suspension of the current collector by using a variable stiffness device. Specifically, the original suspension with constant stiffness is replaced by two facing air springs. Figure 6 presents the prototype of the new pantograph together with its compliance characteristic. Notably, by changing the pressure resistance, the peak frequency of this pantograph can be controlled to adapt the dominant frequency of the catenary irregularity.

In a high-frequency domain, the current collector deforms elastically because of the drastically oscillating contact force, which has a great influence on the pantograph-catenary interaction. Collina et al. [27] studied the performances of different types of current collectors by considering different levels of catenary irregularity (Fig. 7). The relationship between the contact loss ratio and the elastic deformation effects has been analyzed. Their studies helped clarify that a higher complexity in the structure and shape of the current collector corresponds to a higher number of deformable modes in the same frequency range and the horns play a significant role in the position of the first natural frequencies. Figure 7(b) shows that, with the lumped parameter model adopted in their simulation, the contact loss percentage ranges from 0% to 1.5%. By contrast, considering the current collector deformability in the model, the contact loss percentage ranges from 0.3% to 3%. The differences between these two pantograph models in terms of the contact loss ratio increases with the level of irregularity (Fig. 7(b)).

3 System dynamic properties of the pantograph and catenary

Controlling the sensitive parameters that influence performance, with the aim reducing the oscillation of the contact

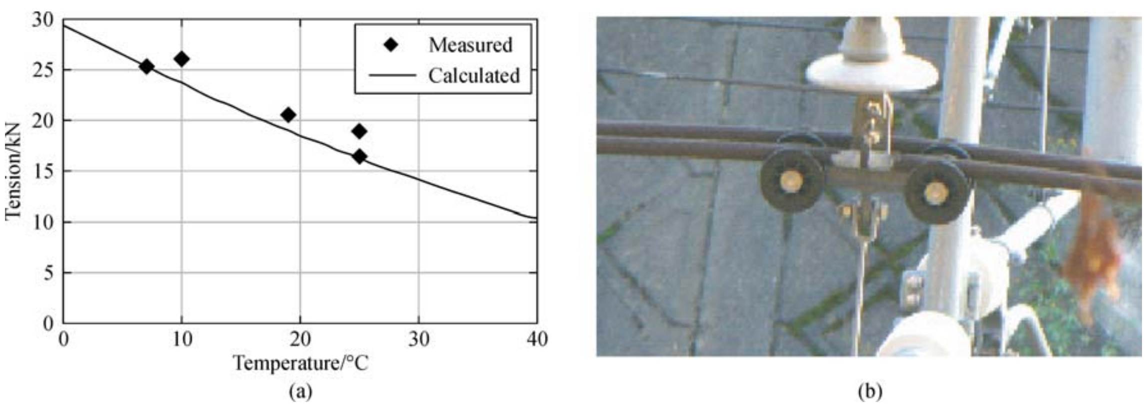

Fig. 5 Temperature-induced tension decreasing in the catenary and the solution. (a) Messenger wire's tension versus temperature; (b) messenger wire supporting pulleys

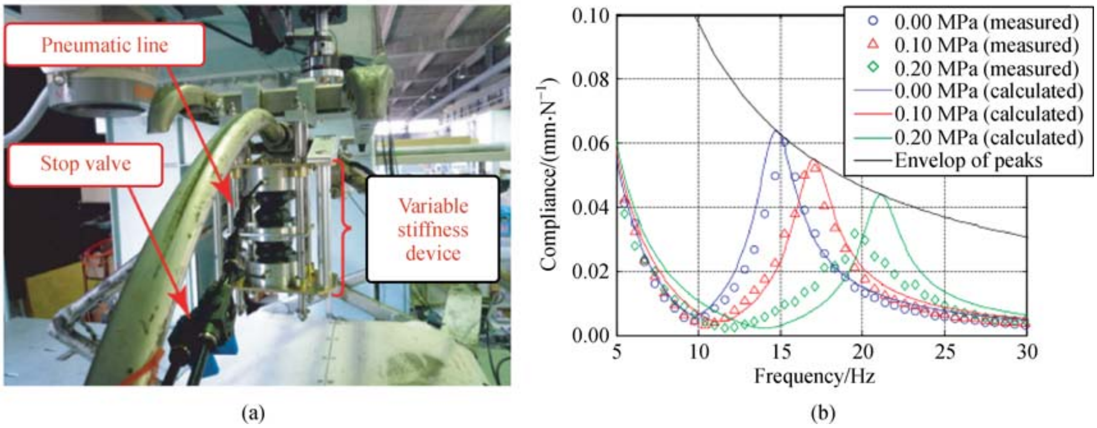

Fig. 6 Variable stiffness device for pantograph suspension. (a) Collector equipped with a variable stiffness device; (b) estimation of the compliance

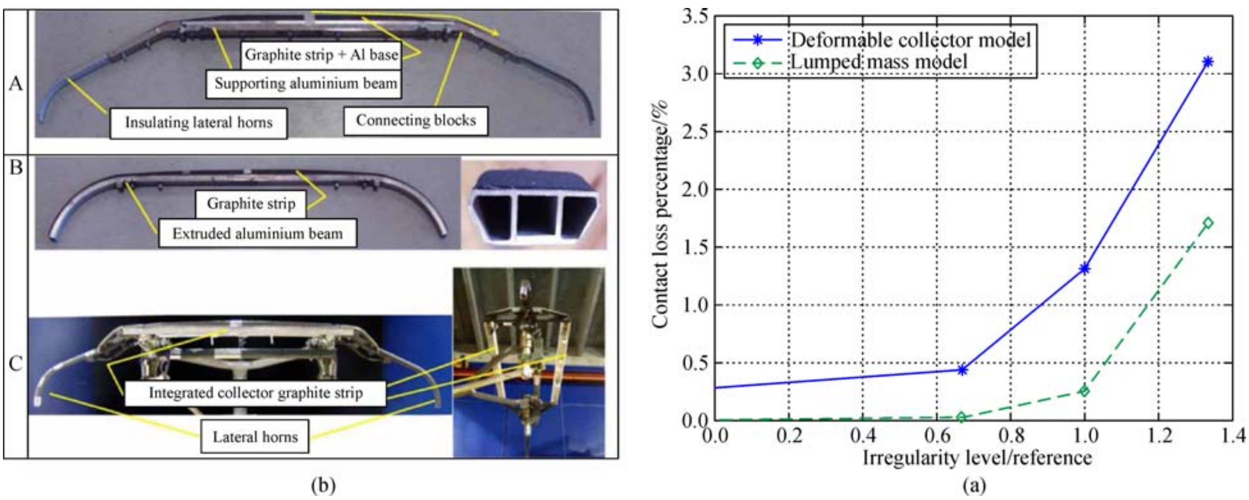

Fig. 7 Contact loss ratio versus catenary irregularities, considering different kinds of collector. (a) Different type of current collectors; (b) elastic deformation effects of current collectors to pantograph-catenary interaction

force, is an important target of researching pantograph and catenary interaction. Present studies have shown that the variation of contact force between the pantograph and catenary mainly depends on the train running speed. In addition, the elastic wave propagated along the catenary also has a significant influence, especially when multiple pantographs are in operation.

3.1 Estimates of damping and properties of the elastic wave

As mentioned in the Introduction, when excited by a moving pantograph at the discontinuous node of the contact wire, the catenary vibrates with the elastic wave propagating along the catenary wires. Due to the structural damping, the wave energy attenuates with the increase of propagating distance. As a result, we review the studies of catenary damping before discussing the characteristics of wave propagation.

3.1.1 Damping

The catenary is a very lightly damped elastic system that always vibrates with low frequency, and even small dissipative effects may significantly affect the pantograph-catenary interaction [28]. Some studies concern the catenary damping. In particular, Cho et al. [29] determined the damping ratios of a railway contact wire by using wavelet transforms. In addition, Bianchi et al. [30] introduced the modal damping to construct a viscosity matrix for full model transient analysis. In their pantograph-catenary dynamic software OSCAR, the Rayleigh damping can be compensated to the modal damping, in order to obtain desired damping effects. Subsequently, with the damping ratios measured from catenary frequency response functions, Vo Van et al. [31] obtained a Rayleigh damping curve; however, the fitted curve is found to give un-reasonable damping effects compared with the experimental signals. Consequently, the fitted curve was combined with the modal damping to give the damping configuration suggested by Bianchi et al. [30]. The studies done by Bianchi et al. [30] and Vo Van et al. [31] are contributive, but the final combined catenary damping configuration they proposed cannot be easily accommodated by other existing software. As a result, Zou et al. [32] proposed a method of a complex Morlet continuous wavelet transform to identify the catenary modal parameters. With the experimental catenary displacement history, the Rayleigh damping coefficients are determined by an iterative simulation as well. Seen from his studies, the damping ratio is about 1% for the frequency range below 2 Hz. For the Rayleigh damping used in the finite element simulation, the mass and stiffness proportional coefficients are approximated at 0.02845 and 0.00274, respectively.

Another contributive study is that from Nåvik et al. [33], who identified the system damping in existing railway catenary systems via an output-only modal analysis of the acceleration time series, which are sampled directly on three different catenary sections. The covariance-driven stochastic subspace identification method is used, and both the ambient vibration and vibration just after the train has passed are considered. Aside from the damping ratios, the unknown Rayleigh coefficients, which correlated to the modal damping ratios with over-determined matrix equations, are obtained for all three catenary sections. For all the investigated catenary sections, the amount of damping relatively decreases rapidly when the frequency increases. In addition, differences of the damping estimates are found between ambient and post-passage as well as between different catenary sections. For the Rayleigh damping, Fig. 8 shows that comparing the damping of the different catenary sections, the estimates from the ambient responses are highly consistent. However, greater differences are observed in the post-passage results, specifically at lower frequencies, whereas the damping at higher frequencies is similar among the catenary sections.

3.1.2 Elastic wave speed and propagation

When the running speed of the pantograph reaches or even exceeds the velocity of the catenary wave propagation, a clear boundary exists between the interrupted and uninterrupted zones upon the catenary. The deformation pattern of the contact wire is similar to the Mach cone in aerodynamics, in which case the uplift of the wire abruptly changes around the contact point and the strain level increases significantly or even becomes plastic. Both increasing the tension of the catenary wire and decreasing its mass per unit length can relieve the abrupt changing of catenary responses. However, increasing the tension reduces the allowance for the increment of stress and also has the risk of breaking off the catenary. In addition, decreasing the mass per unit length increases the transmission resistance of the wire, and consequently, the transmission losses would be increased.

Briefly, the electrified HST has a limit of running speed corresponding to the wave propagation velocity of the catenary. To clarify this speed limit, Park et al. [34] first analyzed the vibration measurements by using the Gabor transform and then determined the catenary wave velocities in accordance with both the time delay of wave

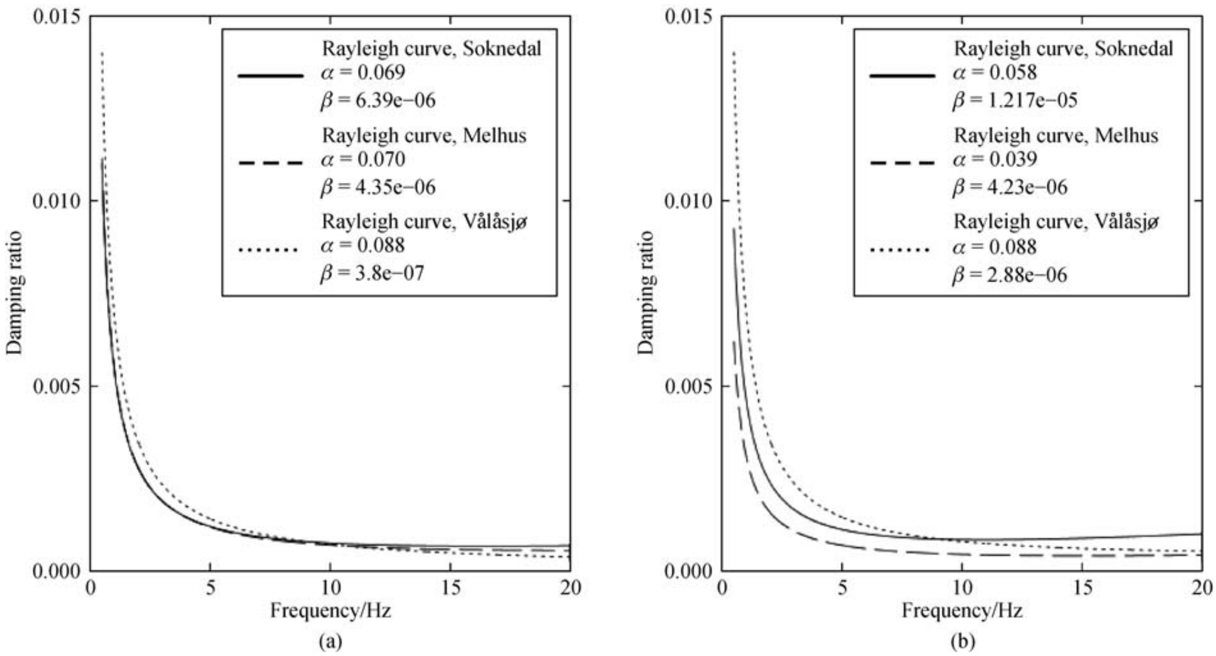

Fig. 8 Rayleigh curve fits for all investigated catenary sections of Soknedal, Melhus, and Vålåsjø. (a) Ambient; (b) post-passage

ridges and the correlation function of wavelet transform coefficients. In addition, Zou et al. [35] utilized the displacement contour of catenary uplift to identify the group velocity of the catenary. He also concluded that calculating the group velocity by treating the contact wire in the overhead-wire system as a single string or beam overestimates the result with a relative error of approximately 13.21%.

For the elastic wave propagating along the catenary, Zou et al. [35] determined the wave propagation pattern on an indoor catenary with three spans. With the displacement contour presented in Fig. 9, a clear rhombus can be seen, in which the vertexes of the rhombus in the contour plot indicate the existence of a local disturbance. The lower diagram in Fig. 9 gives the displacement history of a monitor located at 110 m, in which the local peaks can be well interpreted by the wave propagation. For example, when time elapses to 1.2 s, the right traveling wave reaches the monitor after reflecting at the catenary right end with an opposite phase and consequently stirs up a positive displacement peak.

Meanwhile, Hayasaka [36] used a damping device equipped in the catenary overlap section to reduce the wave reflection. For the damping coefficients of his damper, they are optimized in accordance with the impedance matching of wave guides. For the contact force variation between pantograph and catenary due to the elastic wave, Aboshi and Manabe [37] claimed that the variation has four patterns, which are related to the span length, the space distance between droppers, the wind turbulence, and the irregularity of the contact wire. Some contact force variation mechanism has been presented in his work, but its validation and verification deserve more research attention.

3.2 Dynamics concerning multiple-pantograph operation

Sometimes, more than eight vehicles are grouped into a train to improve the capability of transportation. As a result, the limited capability of a single pantograph requires multiple pantographs put into operation. In this case, the performance of the rear pantograph is feasible to be interrupted by the catenary elastic wave excited by the front ones.

By changing the running speeds and the space distance between pantographs, Manabe and Fujii [38] studied the resonance of pantograph and catenary. The resonance phenomenon, which is identified by the variation of uplift displacement of the rear pantograph, can be degraded by installing a damping device onto the pantograph. Liu et al. [39] focused on the multiple-pantograph operation and found the periodical variation of the performance of the rear pantograph (Fig. 10). To improve the train running speed on the existing soft catenary, the sane author suggested the use of an insulated front pantograph in another study to improve the rear pantograph's performance at high speed, given that the insulated front pantograph producing favorable elastic wave propagated along the catenary [40].

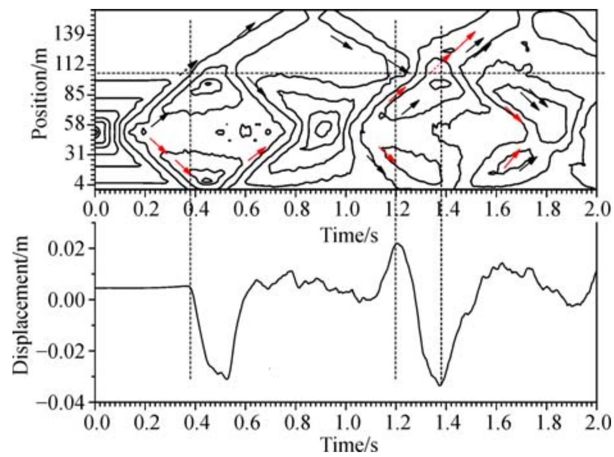

Fig. 9 Wave propagating pattern in the catenary uplift contour and a local displacement history

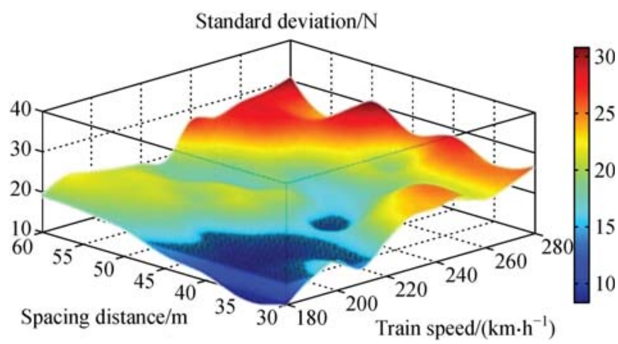

Fig. 10 Periodical variation of the contact force standard deviation of the rear pantograph

Moreover, Zhou [41] claimed that the phase difference between the rear pantograph's uplift and the catenary vibration at a certain position behind the front pantograph is the key factor influencing the performance of the rear pantograph. He also suggested the following formula to calculate a favorable space distance L_g between two pantographs:

$$L_g = (2k+1)\frac{\gamma L_s}{\alpha},\ k = 1,2,3,..., \tag{1}$$

where L_s is the span length, and γ represents a dimensionless ratio between the running speed of the pantograph and the wave propagation velocity of the catenary. Notably, α is the correction coefficient introduced to extend the application of Eq. (1) to different types of catenary, such as the simple and stitched catenary. The studies of Zhou [41] and Liu et al. [39,40] show that the performances of pantograph and catenary system with two or more pantographs in operation depend on the properties of the catenary wave. However, the mechanism of elastic wave interrupting the contact force between the pantograph and catenary is still not comprehensible enough to give a quantitative estimation of contact force variation.

4 Environmental influences on pantograph and catenary performance

The moving pantograph comes into contact with the still catenary under the application of an uplift force. With a low running speed, the disturbances both from wind turbulence and vehicle vibration caused by the irregularities of railway track are ignorable. However, with the increasing running speed, these disturbances become significant, and the resulted drastically varied contact force degrades the performance of pantograph and catenary systems and even induces an accident.

4.1 Wind-induced contact wire offset

As mentioned above, the catenary is a very lightly damped elastic system and always vibrates with low frequency. As a result, especially in the gale region, the wind turbulence always offsets the contact wire from its static position and degrades the system performance [42]. Occasionally, the vibration instability occurs, or even the normal operation of HST can be interrupted. Compared with the pantograph, the investigations of the aerodynamics of catenary under wind turbulence are not very thorough, and most of the related studies are still in an exploratory stage. In particular, some researchers reproduced the wind history by using empirical wind spectra [43]. These approximated wind profiles always differ from the real profiles in environment. To overcome this kind of shortcut, a special catenary for field test use can be seen outdoor in the gale region in China. With the measurements of real wind profiles and the wind-induced responses of the catenary, the design and maintenance of electrical railway catenary can be implemented in a more reasonable way.

4.2 Aerodynamic characteristics of the pantograph

In the high-speed case, wind turbulence not only contributes to the mean but also to the variation of uplift force of the pantograph. To investigate the aerodynamic characteristics of a high-speed pantograph, Guo et al. [44] analyzed the vortex shedding from the pantograph by using the detached eddy simulation technology (Fig. 11), and found that the strength and frequency of the shed vortex greatly influence the aero lift force of the pantograph. When the train speed reaches 350 km/h, the vortex magnifies the amplitude of force variation by more than 110%.

Fig. 11 Vortex contour after pantograph at 350 km/h

During 2000 to 2014, Ikeda and his group [45–53] published serials of their achievements related to the aerodynamic optimization of pantograph. By using the computational fluid dynamics and wind tunnel test and noise measurement, they developed a new pantograph, namely, PEGASUS (Fig. 12). To improve the pantograph performance, they adopted the active suspension device

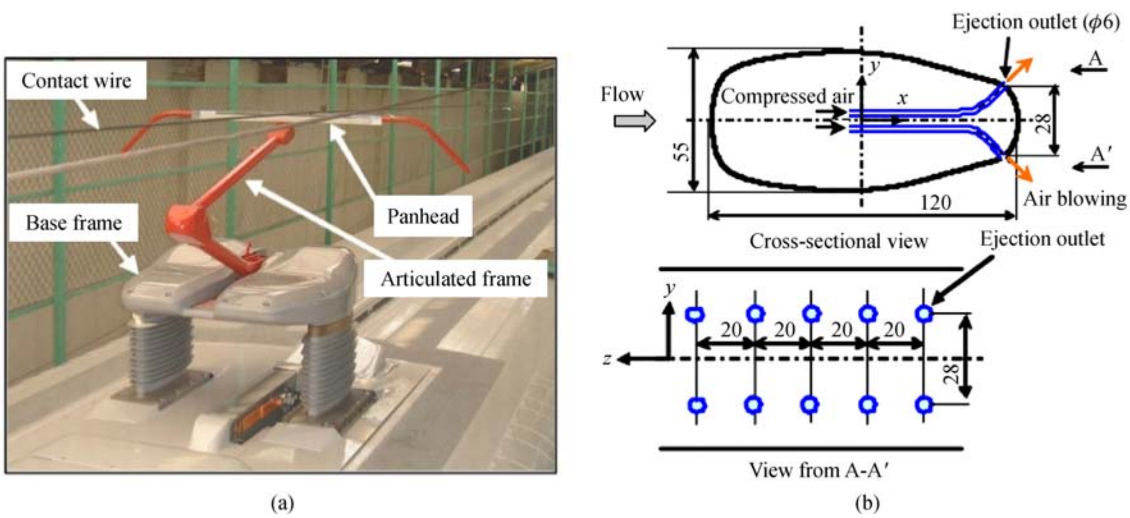

Fig. 12 Pantograph PEGASUS for Shinkansen. (a) PEGASUS; (b) schematic for flow control technology (unit: mm)

together with the flow control technology, such as air blowing and jet ejection. Figure 12(b) presents a panhead model with ejection outlets located on the top and bottom sides of the model near its trailing edge. The lift force is intended to be controlled by blowing air from the single side of the panhead.

In Italy, by using wind tunnel test, the aerodynamic characteristics of different types of current collectors (Fig. 13) are investigated by Bocciolone et al. [54]. After generating the aero forces in accordance with the quasi-static theory, the authors assessed the performance of each current collector in the pantograph-catenary interaction simulation. The authors also suggested that, when seeking an optimization of the collector profile, the first aim is to reduce the drag coefficient. However, if the lift coefficient derivative is too high, then the decreasing drag does not give the expected improvement on the system performance.

The aerodynamic noise originates not only from the pantograph but also from the pantograph recess mounted in the roof of the vehicle. Noger et al. [55] conducted serial tests for a 1/7 scaled model in a low-subsonic wind tunnel. Their results show that the rear vertical face of the recess is proven to be the most complex and turbulent region and is also the origin of the most important noise generation. However, adding fences to the upstream hood could remove the reattachment point inside the recess downstream. As a result, the intensity of the downstream shear layer turbulence is decreased, consequently decreasing the broadband noise level.

4.3 Disturbance from the environment

Regarding the studies of wind disturbance on both the catenary and pantograph, Bouferrouk et al. [56] adopted the aerodynamic admittance theory to study the wind-induced offset on pantograph. By using the wind measurement spectrum, Vo Van et al. [57] reproduced time-varying vertical forces to study the aerodynamic effects on pantograph-catenary interaction. The authors pointed out that the aerodynamic irregularity only affects the mean component of the contact force and has nothing to do with the contact force standard deviation. Their conclusion differs from that presented by Bocciolone et al. [54], who claimed that the wind turbulence not only contributes to the mean but also to the variation of uplift force of the pantograph. With the quasi-static aerodynamic force applied on the high-speed railway catenary, Song et al. [58] studied the wind-induced vibration of the pantograph and catenary system. In addition, due to the existence of the groove on contact wire cross section, both the wind speed and the attack angle exert a significant effect on the catenary vibration and consequently on the pantograph-catenary interaction. For the disturbance from vehicle vibration, Pombo et al. [59–61] indicated that, due to the filtering effects of the vehicle suspension, the vehicle vibration, which is mainly caused by the irregularity of the railway track, has a slight influence on the performance of the pantograph and catenary system.

5 Conclusions and future prospect

The application of electrified railway directly promotes the studies of pantograph and catenary. With the increase of the HST running speed, the operational conditions for a pantograph-catenary system have changed significantly. Before performing further studies, sorting out the related studies is necessary to seek a possible breakthrough. In this paper, studies concerning the dynamics of pantograph and catenary are summarized from three aspects: The dynamic characteristics of components, the system dynamic properties, and the environmental influences on pantograph and catenary performance.

Factors that affect the performance of pantograph and catenary can be classified into static and dynamic aspects. The vertical elasticity within a catenary span plays a

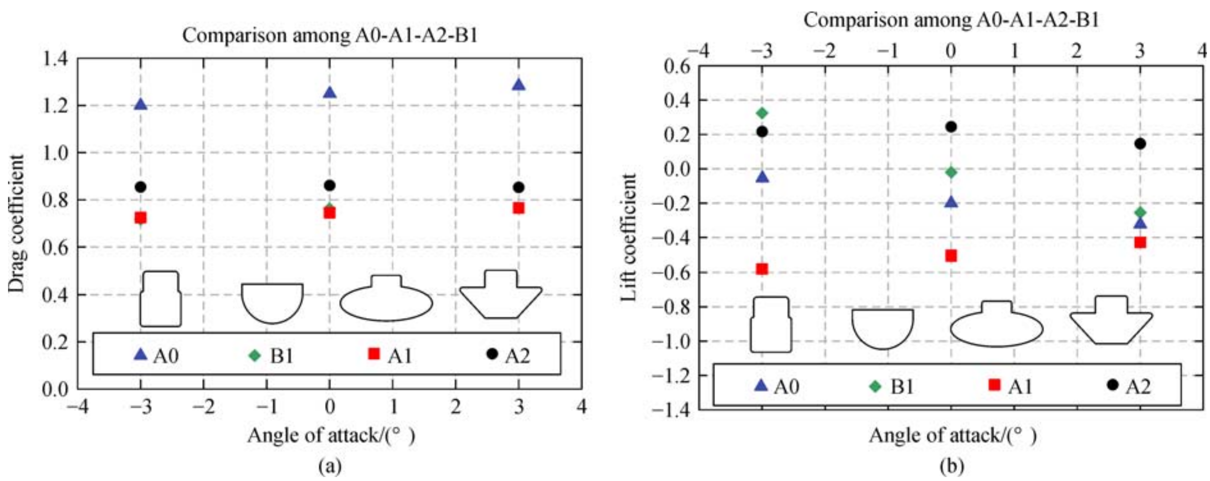

Fig. 13 Aerodynamic coefficients of the collector section profile. (a) Drag coefficient; (b) lift coefficient

critical role among the static factors and mainly depends on the tension of the catenary. In addition, the structural configuration and the geometry of the catenary have influence on it too. For the dynamic aspect, the system performance is mainly affected by the elastic wave and the relationship of natural frequencies between the pantograph and catenary. Briefly, the interaction of the pantograph and catenary is affected by many factors, and many factors correlate to each other in a complex way. Therefore, future studies must find ways to explain the mechanism of contact force variation but not just to interpret the apparent phenomenon. Possibly, it can be achieved by simplifying the pantograph and catenary interaction into a moving load problem. After extending the fundamental achievements to the real pantograph and catenary system, the most sensitive factors affecting contact force could be clarified and then used to control the performance of the pantograph and catenary.

Meanwhile, knowledge of the characteristics of external flow around the pantograph and catenary is required to clarify the key components affecting the aerodynamic performance and noise. As the basic approaches to investigate the aerodynamics, the technology of producing a scaled or full-scale model of the pantograph and catenary for wind tunnel test, the meshing generation, and the turbulence modeling for flow field outside complex geometry deserve more attention. Moreover, the active and flow controlling technologies, i.e., shape optimization and vortex generator, can also be used to improve the system performance. To simulate the pantograph-catenary interaction with accurate operational conditions, developing a computational platform that accommodates both track-train and pantograph-catenary interactions and also the environment-induced couplings is necessary. On the basis of this kind of platform, the theory of matching mechanical impedance (or admittance) and the principle of power flow can be adopted to study the distribution and transmission of system energy. Eventually, the parameters of the pantograph and catenary can be designed and assessed in a more reasonable approach.

Remarkably, the pantograph and catenary interact in a multi-physical field. A slight disturbance of the structural parameters may lead to dramatic changes of performance index in different categories. However, the related studies are still in the preliminary stage. As a first step, the relationship between the generation of arc and the variation of contact force could be investigated. The second key point lies on the heat-induced friction/wear of the contact materials. To date, the task of conducting such studies is full of challenges, especially when innovations of testing and measurement technologies are in great demand.

Acknowledgements The authors are grateful for the support provided by the National Key Research and Development Plan-Specific Project of Advanced Rail Transportation (Grant Nos. 2016YFB1200401-102B and 2016YFB1200506), the National Natural Science Foundation of China (Grant No. 51475391), and the Project of Research and Development of Science and Technology from the China Railway Corporation (Grant No. 2017J008-L).

References

1. Yang G W, Wei Y J, Zhao G L, et al. Research of key mechanics problems in high speed train. Advances in Mechanics, 2015, 45(1): 217–460 (in Chinese)
2. Kubo S, Kato K. Effect of arc discharge on the wear rate and wear mode transition of a copper-impregnated metalized carbon contact strip sliding against a copper disk. Tribology International, 1999, 32 (7): 367–378
3. Yamashita C, Sugahara A. Wear modes of contact wire and contact strip under electric current condition. Quarterly Report of RTRI, 2014, 55(2): 67–72
4. Collina A, Melzi S. Effect of contact strip-contact wire interaction on current transfer at high sliding speed in the mid-high frequency range. In: Proceedings of the AITC-AIT Conference. Parma, 2006
5. Ding T, Chen G X, Bu J, et al. Effect of temperature and arc discharge on friction and wear behaviors of carbon strip/copper contact wire in pantograph-catenary systems. Wear, 2011, 271(9–10): 1629–1636
6. Midya S. Electromagnetic interference in modern electrified railway systems with emphasis on pantograph arcing. Dissertation for the Doctoral Degree. Stockholm: Uppsala University, 2008
7. Usuda T. Estimation of wear and strain of contact wire using contact force of pantograph. Quarterly Report of RTRI, 2007, 48(3): 170–175
8. Shibata K, Yamaguchi T, Mishima J, et al. Friction and wear properties of copper Caron RB ceramics composite materials under dry condition. Tribology Online, 2008, 3(4): 222–227
9. Collina A, Melzi S, Facchinetti A. On the prediction of wear of contact wire in OHE lines: A proposed model. Vehicle System Dynamics, 2002, 37(Suppl 1): 579–592
10. Bucca G, Collina A. A procedure for the wear prediction of collector strip and contact wire in pantograph-catenary system. Wear, 2009, 266(1–2): 46–59
11. Ying W, Liu Z G, Ke H, et al. Pantograph-catenary surface heat flow analysis and calculations based on mechanical and electrical characteristics. Journal of the China Railway Society, 2014, 36(7): 36–43 (in Chinese)
12. Ying W, Liu Z G, Fan F Q, et al. Review of research development of pantograph-catenary arc model and electrical characteristics. Journal of the China Railway Society, 2013, 35(8): 35–43 (in Chinese)
13. Wu G, Zhou Y, Lei D, et al. Research advances in electric contact between pantograph and catenary. High Voltage Engineering, 2016, 42(11): 3495–3506 (in Chinese)
14. Vesnitskii A I, Metrikin A V. Transition radiation in one-dimensional elastic systems. Journal of Applied Mechanics and Technical Physics, 1992, 33(2): 202–207
15. Lee K, Chung J. Dynamic analysis of a hanger-supported beam with a moving oscillator. Journal of Sound and Vibration, 2013, 332(13): 3177–3189
16. Lopez-Garcia A, Carnicero A, Torres V, et al. The influence of cable

slackening on the stiffness computation of railway overheads. International Journal of Mechanical Sciences, 2008, 50(7): 1213–1223

17. Cho Y H, Lee K, Park Y, et al. Influence of contact wire pre-sag on the dynamics of pantograph-railway catenary. International Journal of Mechanical Sciences, 2010, 52(11): 1471–1490
18. Cho Y H. Numerical simulation of the dynamic responses of railway overhead contact lines to a moving pantograph, considering a nonlinear dropper. Journal of Sound and Vibration, 2008, 315(3): 433–454
19. Morikawa T. Investigation of stress of contact wire clamped with steady arms under a moving constant force passing by. Quarterly Report of RTRI, 2000, 41(4): 163–168
20. Amari S, Tsunemoto M, Kusumi S, et al. Evaluation of resistance at supporting pulley of messenger wire and its influence on current collection characteristics. Quarterly Report of RTRI, 2009, 50(3): 137–143
21. Sugahara A. Reduction of contact wire strain near dead sections by considering sliding surface level differences. Quarterly Report of RTRI, 2004, 45(2): 74–79
22. Park T J, Han C S, Jang J H. Dynamic sensitivity analysis for the pantograph of a high-speed rail vehicle. Journal of Sound and Vibration, 2003, 266(2): 235–260
23. Kim J W, Chae H C, Park B S, et al. State sensitivity analysis of the pantograph system for a high-speed rail vehicle considering span length and static uplift force. Journal of Sound and Vibration, 2007, 203(3–5): 405–427
24. Kim J W, Yu S N. Design variable optimization for pantograph system of high-speed train using robust design technique. International Journal of Precision Engineering and Manufacturing, 2013, 14(2): 267–273
25. Pombo J, Ambrósio J. Influence of pantograph suspension characteristics on the contact quality with the catenary for high speed trains. Computers & Structures, 2012, 110–111: 32–42
26. Yamashita Y, Ikeda M. Upgrading pantograph performance using variable stiffness devices. Quarterly Report of RTRI, 2010, 51(4): 214–219
27. Collina A, Lo Conte A, Carnevale M. Effect of collector deformable modes in pantograph-catenary dynamic interaction. Proceedings of the Institution of Mechanical Engineers, Part F: Journal of Rail and Rapid Transit, 2009, 223(1): 1–14
28. Bruni S, Ambrosio J, Carnicero A, et al. The results of the pantograph-catenary interaction benchmark. Vehicle System Dynamics, 2015, 54(3): 412–435
29. Cho Y H, Lee J M, Park S Y, et al. Robust measurement of damping ratios of a railway contact wire using wavelet transforms. Key Engineering Materials, 2006, 321–323: 1629–1635
30. Bianchi J P, Balmès E, Roches G V D, et al. Using modal damping for full model transient analysis: Application to pantograph/catenary vibration. In: Proceedings of ISMA2010-International Conference on Noise and Vibration Engineering including USD2010. Leuven, 2010, 20–22
31. Vo Van O, Balmes E, Lorang X. Damping characterization of a high speed train catenary. International Symposium on Dynamics of Vehicles on Roads and Tracks, 2015, 1505–1512
32. Zou D, Zhang W H, Li R P, et al. Determining damping characteristics of railway overhead wire system for finite element analysis. Vehicle System Dynamics, 2016, 54(7): 902–917
33. Nåvik P, Rønnquist A, Stichel S. Identification of system damping in railway catenary wire systems from full-scale measurements. Engineering Structures, 2016, 113: 71–78
34. Park S Y, Jeon B U, Lee J M, et al. Measurement of low-frequency wave propagation in a railway contact wire with dispersive characteristics using wavelet transform. Key Engineering Materials, 2006, 321–323: 1609–1615
35. Zou D, Zhou N, Li R P, et al. Experimental and simulation study of wave motion upon railway overhead wire system. Proceedings of the Institution of Mechanical Engineers, Part F: Journal of Rail and Rapid Transit, 2016, 231(8): 934–944
36. Hayasaka T. Effect of reduced reflective wave propagation on overhead contact lines in overlap section. Quarterly Report of RTRI, 2004, 45(2): 68–73
37. Aboshi M, Manabe K. Analyses of contact force fluctuation between catenary and pantograph. Quarterly Report of RTRI, 2000, 41(4): 182–187
38. Manabe K, Fujii Y. Overhead system resonance with multi-pantographs and countermeasures. Railway Technical Research Institute, Quarterly Reports, 1989, 30(4): 175–180
39. Liu Z, Jönsson P A, Sebastian S, et al. Implications of the operation of multiple pantographs on the soft catenary systems in Sweden. Proceedings of the Institution of Mechanical Engineers. Part F, Journal of Rail and Rapid Transit, 2015, 53(3): 341–346
40. Liu Z, Jönsson P A, Stichel S, et al. On the implementation of an auxiliary pantograph for speed increase on existing lines. Vehicle System Dynamics, 2016, 54(8): 1077–1097
41. Zhou N. Pantograph and catenary interaction with the train speed beyond 350 km/h. Dissertation for the Doctoral Degree. Chengdu: Southwest Jiao Tong University, 2012
42. Li R, Zhang W, Zhou N, et al. Influence of a high-speed train passing through a tunnel on pantograph aerodynamics and pantograph-catenary interaction. Proceedings of the Institution of Mechanical Engineers, Part F: Journal of Rail and Rapid Transit, 231: 198–210
43. Li R, Zhou N, Zhang W, et al. Fluctuating wind field and wind-induced vibration response of catenary based on AR model. Journal of Traffic and Transportation Engineering, 2013, 13(4): 56–62 (in Chinese)
44. Guo D, Yao S, Liu C, et al. Unsteady aerodynamic characteristics of high-speed pantograph. Journal of the China Railway Society, 2012, 34(11): 16–21
45. Suzuki M, Ikeda M, Yoshida K. Study on numerical optimization of cross-sectional panhead shape for high-speed train. Journal of Mechanical Systems for Transportation and Logistics, 2008, 1(1): 100–110
46. Suzuki M, Ikeda M, Koyama T. Flow control for pantographs using air intake and outlet. Journal of Mechanical Systems for Transportation and Logistics, 2008, 1(3): 272–280
47. Ikeda M, Manabe K. Development of low noise pantograph with passive lift suppression mechanism of panhead. Quarterly Report of RTRI, 2000, 41(4): 177–181
48. Ikeda M, Takaishi T. Perforated pantograph horn Aeolian tone suppression mechanism. Quarterly Report of RTRI, 2004, 45(3):

169–174

49. Takaishi T, Ikeda M. Numerical method for evaluating aeroacoustic sound sources. Quarterly Report of RTRI, 2005, 46(1): 23–28
50. Ikeda M, Suzuki M, Yoshida K. Study on optimization of panhead shape possessing low noise and stable aerodynamic characteristics. Quarterly Report of RTRI, 2006, 47(2): 72–77
51. Ikeda M, Yoshida K, Suzuki M. A flow control technique utilizing air blowing of modify the aerodynamic characteristics of pantograph for high speed train. Journal of Mechanical Systems for Transportation and Logistics, 2008, 1(3): 264–271
52. Ikeda M, Mitsumoji T. Evaluation method of low frequency aeroacoustic noise source structure generated by shinkansen pantograph. Quarterly Report of RTRI, 2008, 49(3): 184–190
53. Mitsumoji T, Sato Y, Ikeda M, et al. A basic study on aerodynamic noise reduction techniques for a pantograph head using plasma actuators. Quarterly Report of RTRI, 2014, 55(3): 184–189
54. Bocciolone M, Resta F, Rocchi D, et al. Pantograph aerodynamic effects on the pantograph-catenary interaction. Vehicle System Dynamics, 2006, 44(Suppl 1): 560–570
55. Noger C, Patrat J C, Peube J, et al. Aeroacoustical study of the TGV pantograph recess. Journal of Sound and Vibration, 2000, 231(3): 563–575
56. Bouferrouk A, Baker C J, Sterling M, et al. Calculation of the crosswind displacement of pantographs. In: Proceedings of BBAA VI International Colloquium on: Bluff Bodies Aerodynamics & Applications. Milano, 2008, 20–24
57. Vo Van O, Massat J P, Laurent C, et al. Introduction of variability into pantograph-catenary dynamic simulations. Vehicle System Dynamics, 2014, 52(10): 1254–1269
58. Song Y, Liu Z, Wang H, et al. Nonlinear analysis of wind-induced vibration of high-speed railway catenary and its influence on pantograph-catenary interaction. Vehicle System Dynamics, 2016, 54(6): 723–747
59. Pombo J, Ambrósio J. Environmental and track perturbations on multiple pantograph interaction with catenaries in high-speed trains. Computers & Structures, 2013, 124: 88–101
60. Pombo J, Ambrósio J, Pereira M, et al. Influence of the aerodynamic forces on the pantograph-catenary system for high speed trains. Vehicle System Dynamics, 2009, 47(11): 1327–1347
61. Pombo J, Ambrosio J. Multiple pantograph interaction with catenaries in high-speed trains. Journal of Computational and Nonlinear Dynamics, 2012, 7(4): 041008